Efficient positronium laser excitation for antihydrogen production in a magnetic field

F. Castelli, I. Boscolo, S. Cialdi, M.G. Giammarchi,

INFN and Università di Milano, via Celoria 16, 20133 Milano, Italy

D. Comparat

Laboratoire Aimé Cotton, CNRS Univ Paris-Sud Bât.505, 91405 Orsay, France

(Dated: November 17, 2018)

Abstract

Antihydrogen production by charge exchange reaction between Positronium (Ps) atoms and antiprotons requires an efficient excitation of Ps atoms up to high-n levels (Rydberg levels). In this study it is assumed that a Ps cloud is produced within a relatively strong uniform magnetic field (1 Tesla) and with a relatively high temperature (100 K). Consequently, the structure of energy levels are deeply modified by Zeeman and motional Stark effects. A two–step laser light excitation, the first one from ground to $n = 3$ and the second from this level to a Rydberg level, is proposed and the physics of the problem is discussed. We derive a simple formula giving the absorption probability with substantially incoherent laser pulses. A 30% population deposition in high-n states can be reached with feasible lasers suitably tailored in power and spectral bandwidth.

I. INTRODUCTION

Some fundamental questions of modern physics relevant to the unification of gravity with the other fundamental interactions such as models involving vector and scalar gravitons and matter anti-matter symmetry (CPT) can be enlightened via experiments with antimatter [1]. In particular, some quantum gravity models claim for possible violations of the equivalence principle of General Relativity in antimatter [2]. Testing the validity of this principle is an important issue, and may involve measurements of the inertial and gravitational mass equality using different experimental settings, for example determining gravitational acceleration on cold atoms [3]. The authors of the present paper are co-proponents of the AEGIS (Antimatter Experiment: Gravity, Interferometry, Spectroscopy) experiment [4, 5] aiming to measure the Earth Gravitational acceleration $\bar{g}$ on a cold and collimated antihydrogen $\bar{H}$ beam.

The production of cold antihydrogen bunches occurs in the charge transfer of a cloud of Rydberg excited positronium atoms (Ps) (stored in a magnetic trap) with a bunch of cold antiproton $\bar{p}$ by means of the reaction $Ps^* + \bar{p} \rightarrow \overline{H} + e^-$ [6]. Ps atoms and antiprotons are prepared inside a cryostat. Here we will focus on the excitation at high quantum levels of the Ps atomic cloud.

The $\bar{H}$ formation process has to be very efficient. The number antihydrogen atoms produced in the charge exchange reaction is expressed, with obvious notation, as $N_{\bar{H}} = \rho\, N_{Ps}\, N_{\bar{p}}\, \sigma/A$ where ρ is the overlap factor between the trapped $\bar{p}$ and the Ps cloud with transverse area A. Since the cross section σ depends on the fourth power of the principal quantum number n of the excited Ps [6] ($\sigma \propto n^4 \pi a_0^2$, where a_0 is the Bohr radius), n can be chosen to be in the range from 20 to 30. As we shall see later, higher n values should be avoided in order to reduce ionization losses due to stray fields and dipole-dipole interactions. Incidentally, the higher the n-value the longer the Ps lifetime.

Positronium excitation to these high-n levels (the so-called Rydberg levels) can be obtained either via collisions or via photon excitation. In reference [6] Ps excitation was proposed and tested through Cs excitation by light and a successive charge exchange reaction with positrons. We propose (in the AEGIS experiment) a direct Ps excitation by a two step light excitation using two simultaneous laser pulses with different wavelengths. This excitation process should be very efficient, more controllable and of simpler and more

compact experimental set up than the previous one.

An efficient way of producing Ps atoms is by letting positrons impinge on a proper porous silica surface [7]. The Ps exiting the target surface forms an expanding cloud at a temperature up to 100 K, and the cloud is constrained by a magnetic trap with a relatively strong field $\vec{B}$ of about 1 Tesla [4]. Ps atom resonances will then be broadened by Doppler effect because the atoms have random velocities of the order $v \sim 10^5 \, m/s$ at the 100 K reference temperature. Moreover the sublevels of a Rydberg excited state will be mixed and separated in energy by the motional Stark effect and by linear and quadratic Zeeman splitting. Because of these effects the transition will be from ground or from a low–excited level to a broadened Rydberg level–band. This last is in fact the relevant characteristic which distinguishes the Ps laser excitation from the usual atomic excitation to Rydberg levels; therefore it requires a careful theoretical analysis and a suitable experimental setup. The characteristics of laser pulses in terms of power and spectral bandwidth must be tailored to the geometry, the Rydberg level–band and the timing of the Ps expanding cloud. The laser power must be enough to ensure the whole Ps cloud excitation within a few nanoseconds.

The interest on laser Ps excitation started with theoretical studies on the delayed annihilation [8] induced by excitation towards p and d states using nanosecond or longer pulses. Subpicosecond pulses of very intense laser radiation were proposed and analyzed both for spectroscopic studies and for antihydrogen formation by the charge exchange process [9], calculating population deposition on low energy states essentially by two-photon absorption. Generally, these studies did not consider Rydberg states, nor the presence of a magnetic field. The problem of Ps Rydberg excitation with nanosecond laser pulses in a magnetic environment was faced and experimentally performed in Ref. [10] for n up to 19, but in a different regime with respect to ours, as discussed below.

The photo–excitation of Ps to the Rydberg band requires photon energies close to 6.8 eV. Laser systems at the corresponding wavelength (≈ 180 nm) are not commercially available, hence a two–step excitation was required. We are taking into consideration the transition from the ground state to $n = 3$ state ($\lambda = 205$ nm), and then to high–n levels ($\lambda \sim 1670$ nm). This choice seems more adequate than the other possible two step sequence $1 \rightarrow 2$ and $2 \rightarrow$ high-n because the level $n = 2$ has a three time shorter lifetime than the the $n = 3$ level (3 ns against 10.5 ns) and, in addition, population loss becomes dynamically relevant. The two photon excitation $1 \rightarrow 2 \rightarrow n$ was reported in Ref. [10].

A commercial Dye–prism laser (optically pumped by the second harmonic of a Q–switched Nd:YAG laser) coupled to a third harmonic generator can provide the 205 nm photons for the first transition. The laser for the second transition is yet to be developed and it is being proposed for the AEGIS experiment [4]. In the discussed two–photon excitation we must use a relatively high intensity pulse in order to have an efficient transition process. Since one needs to avoid losses in the excited population due to the short lifetime of the intermediate levels, the pulse time length cannot exceed a few nanoseconds; their expected value is around 5 ns.

We perform the calculation of the excitation process to relate the absorption probability rate to the laser power and its spectral bandwidth characteristics, using a suitable definition of transition saturation fluence.

II. MODELING PS EXCITATION FROM $n = 1$ TO HIGH–n LEVELS

Here we consider a simple theoretical model of Ps excitation to calculate laser saturation fluence and useful bandwidth. The excitation of Ps in high–n state is described as a cascade or a two-step transition: a first step by a resonant excitation from $n = 1$ to $n = 3$, and a second step by a near resonant excitation from $n = 3$ to high–n. The spectral profile of the two laser intensities is characterized by a Gaussian function whose full width at half maximum (FWHM) $\Delta\lambda_L$ is matched to a selected Rydberg level–bandwidth around a definite n state. The broad laser linewidths come along with a coherence time $\Delta t_{coh} = \lambda^2/c\,\Delta\lambda_L$, where λ is the central wavelength of the proper transition. This parameter turns out to be up to three orders of magnitude shorter than the average 5 ns duration of the laser pulses [4], hence we are operating with a completely incoherent excitation for both transitions.

The detailed structure of the optical transition to high–n energy levels of positronium is dominated by:

- the Doppler effect;

- the Zeeman and motional Stark effects,

because their energy contribution is larger than hyperfine and spin–orbit splitting in the experimental conditions. However, the importance of these effects for the effective level

structure is completely different for $n = 3$ and for Rydberg states. As we shall see, while the first transition is marginally affected by Zeeman and Stark effects, the high n levels involved in the second transition are turned into energy bands by Stark effect, strongly affecting the physics of the excitation. Therefore we will treat the two transitions separately.

The challenging problem of Rydberg states of an atom moving in a magnetic field has attracted many experimental and theoretical researches [11]. The Ps atom is a special case because the first order Zeeman effect, *i.e.* the direct interaction between magnetic field and magnetic dipoles, only mixes ortho and para Ps states with $m_S = 0$ without affecting orbital quantum numbers [12]. This interaction energy contribution amounts to $\pm 1.2 \times 10^{-4}$ eV for $B = 1$ T (much lower than the actual Doppler broadening, see below), while the energy of $m_S = \pm 1$ states remain unchanged. The level mixing leads to the well known enhancement of the average annihilation rate of the Ps thermal ground state $n = 1$ [13], leaving in fact only the ortho–Ps states with $m_S = \pm 1$ surviving in the Ps cloud expanding from the silica converter. From the observation that the electric dipole selection rules for optical transitions impose conservation of spin quantum number, and that the broadband characteristics of our laser overlaps the Zeeman splitting, we may conclude that in first approximation this effect does not play any role in the transition. Thus we will concentrate our attention only on the dominant motional Stark effect. As a final note we observe that the quadratic (diamagnetic) Zeeman effect can be discarded because it gives an energy contribution only for higher magnetic fields and high n (being proportional to n^4) [12, 14], hence in a regime where the motional Stark effect dictates the transition structure.

Since Doppler and Stark effects depend on temperature, in the following calculations we select for definiteness the reference temperature of 100 K, which corresponds to the largest Ps cloud exiting the converter, and consequently greater laser powers. This choice ensures a successful Ps excitation with lower temperatures as well.

A.   Excitation from $n = 1$ to $n = 3$

In the first excitation step the Doppler linewidth $\Delta\lambda_D$, scaling as $\sqrt{T}$, turns out to be around 4.4×10^{-2} nm, corresponding to the energy broadening $\Delta E_D \simeq 1.3 \times 10^{-3}$ eV. A motional Stark electric field $\vec{E} = \vec{v} \times \vec{B}$, where $\vec{B}$ is taken for definiteness along the z axis, is induced by the Ps motion within the relatively strong magnetic field $B \sim 1$ T [15] .

This effect splits the sub–levels of the state $n = 3$ in energy and leads to some mixing of quantum numbers m and ℓ, due to the breaking of the axial symmetry of moving Ps atoms. The maximum broadening due to this effect is evaluated as $\Delta\lambda_S \simeq 1.8 \times 10^{-3}$ nm (the total energy width of the sub–level structure amount to $\Delta E_S \simeq 5.3 \times 10^{-5}$ eV) [16], negligible with respect to the Doppler broadening. Therefore we conclude that the width of the transition $1 \to 3$ is dominated by the Doppler broadening, and the laser linewidth must be provided accordingly.

Since Ps excitation is incoherent, the saturation fluence is calculated by a rate equation model (see the Appendix). The excitation probability for unit time is

$$W_{13}(t) = \int d\omega \, \frac{I(\omega, t)}{\hbar \, \omega} \, \sigma_{13}(\omega) \tag{1}$$

where $I(\omega, t)$ is the power spectrum of the laser pulse and the absorption cross section σ_{13} is

$$\sigma_{13}(\omega) = \frac{\hbar \, \omega}{c} \, g_D(\omega - \omega_{13}) \, B_{1 \to 3}(\omega) \tag{2}$$

(c is the vacuum light speed and $\hbar$ is the Planck constant divided by 2π). The function $g_D(\omega - \omega_{13})$ is the normalized lineshape representing the Doppler broadened line, *i.e.* a Gaussian function centered on the transition frequency ω_{13} and with a FWHM corresponding to the Doppler linewidth $\Delta\lambda_D$. The factor $B_{1 \to 3}(\omega)$ is the absorption Einstein coefficient appropriate to the dipole–allowed transition (the frequency dependence is inserted for consistency with the following subsection). In first approximation [15] this coefficient coincides with that of the unperturbed transition $(1, 0, 0) \to (3, 1, m)$ where m can be selected by the laser polarization, specified by the unit vector $\vec{\epsilon}$. Hence one has $B_{1 \to 3}(\omega) = |d_{1 \to 3}|^2 \pi / \varepsilon_0 \hbar^2$ with the electric dipole matrix element $d_{1 \to 3} = \langle \psi_{100} | e \, \vec{r} \cdot \vec{\epsilon} | \psi_{31m} \rangle$ (where e is the electron charge and $\vec{r}$ the position operator) calculated using standard methods from the general theory of radiative transition in atomic physics [17] and the exact Gordon formula [18].

By matching the resonant laser linewidth to the Doppler broadening (aiming to maximize Ps cloud covering in the spectral domain) and assuming for definiteness linear laser polarization along the z axis, from the results of the rate equation theory developed in Appendix (see Eq. (A.5)) we can determine the saturation fluence for the first transition as

$$F_{sat}(1 \to 3) = \frac{c^2}{B_{1 \to 3}} \sqrt{\frac{2 \, \pi^3}{\ln 2}} \cdot \frac{\Delta\lambda_D}{\lambda_{13}^2} = 93.3 \, \mu\text{J/cm}^2 \tag{3}$$

6

This equation gives the lowest pulse fluence needed for reaching transition saturation. The energy of the exciting laser pulse will depend on the laser spot-size (which must overlap the Ps cloud). Assuming a transverse cloud FWHM dimension of $\Delta r = 2.8$ mm (the Ps cloud section of 6 mm^2 of AEGIS proposal) and fixing the fluence value F_0 at the maximum of the transverse Gaussian laser profile as $F_0 = 2F_{sat}$, the laser pulse energy $(E = \pi(F_0/2)(\Delta r/1.177)^2)$ comes out to be $E_I = 16.2\,\mu$J.

B. Excitation from $n = 3$ to Rydberg levels

The physics of the second transition $n = 3 \rightarrow$ high–n is significantly different. The Doppler broadening is practically independent of n and turns out to be around 0.35 nm at 100 K (corresponding to an energy broadening of 1.6×10^{-4} eV), whereas the Stark motional effect turns out to be many times higher, as depicted in Fig. 1.
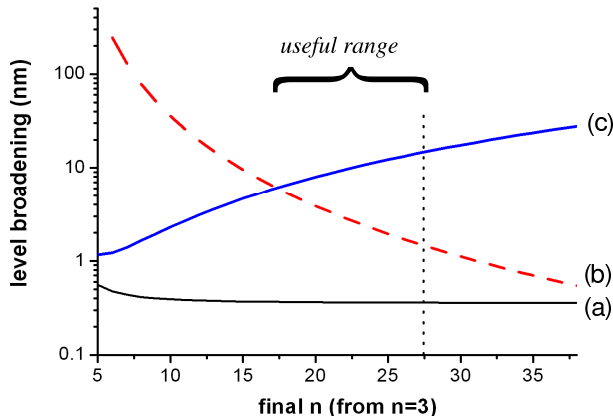

FIG. 1: (Color online) Doppler (a) and Stark (c) line–broadenings as a function of the principal quantum number n for the transition $3 \rightarrow n$. The dashed line (b) shows the energy distance (in nm) between adjacent unperturbed n states. The dotted vertical line is the ionization limit for the lowest sub level. The useful range for Ps Rydberg excitation is indicated.

The effect due to the motional Stark electric field becomes the dominant characteristic of the transition. Because of it, the degenerate high–n levels become fans or manifolds of their n^2 sub–levels with a complete mixing of their m and ℓ sub states, while the mixing between n–levels in Positronium atoms does not occur to a good extent [19]. Owing to the m and ℓ sub–level mixing, these unperturbed quantum numbers are no longer good quantum numbers labelling the states, at variance with the principal quantum number n which retains

its role [10, 15]. The energy width ΔE_S of a fan can be evaluated from the usual theory of the Stark effect, and increases both with the magnetic field and n as

$$
\begin{aligned}
\Delta E_S &= 6\, e\, a_0\, n\, (n-1)\, |\vec{E}(v_\perp)| \\
&= 6\, e\, a_0\, n\, (n-1)\, B\, \sqrt{k_B T/m}
\end{aligned}
\tag{4}
$$

where a_0 is the Bohr radius, $v_\perp = \sqrt{k_B T/m}$ is the positronium atom thermal transverse velocity (m being the positronium mass) and a factor of 2 comes from the fact that the radius of the ground state of a Ps atom is equal to $2a_0$. The broadening $\Delta\lambda_S \simeq \Delta E_S\, \lambda^2/2\pi c\hbar$ of the transition is shown in Fig. 1. It is worth noting that the splitting between adjacent unperturbed energy levels (which energy is $E_n = -13.6\,\text{eV}/2n^2$) decreases with n

$$
\Delta E_n \simeq 13.6\,\text{eV} \cdot \frac{1}{n^3}
\tag{5}
$$

as shown in the figure. Therefore for $n > 16$ the bandwidth filled by the sublevels relative to an n state becomes overwhelmingly greater than the interval between two adjacent n–levels. Thus, at n larger than 16 an interleaving of many sublevels is expected. The range of n levels useful for the charge transfer reaction and efficient $\bar{H}$ formation starts from $n \sim 20$, i.e. in the region of notable level mixing. We would like to remark that our calculations refer to the cases where $\Delta E_S \gg \Delta E_n$ (as it comes out from Fig. 1).

Another effect of the motional Stark electric field that has to be considered is the possible atom ionization: the transition from the bound state to an ionized state occurs from the bottom sub–level of an n–fan (the *red–state* [19]) to the unbound states. This action determines an upper n–level useful for our purpose. The minimum Stark electric field $\vec{E}_{min}$ which induces high ionization probability at the lowest energy $E = E_n - 3ea_0 n\, (n-1)\,|\vec{E}_{min}|$ of the level fan is calculated as [19]

$$
|\vec{E}_{min}| = \frac{e}{16\,\pi\,\varepsilon_0\, a_0^2}\, \frac{1}{9\, n^4} \cdot
\tag{6}
$$

Hence, for $B = 1$ T and for the reference temperature of 100 K, the ionization starts affecting part of the level fan for $n > 27$. This ionization limit, and the useful range for n, are indicated in Fig. 1.

Let us consider the distribution of the sublevels to calculate the $3 \to$ high–n transition probability. For a given n, a uniform distribution of the n^2 fan sublevels within the motional

Stark energy width ΔE_S may be assumed. The number of originally unperturbed n–levels interleaved with that reference n–level within its fan width is approximately (see also Fig. 2)

$$N_n \simeq \frac{\Delta E_S}{\Delta E_n} \simeq n^5 \frac{6 \, e \, a_0}{13.6 \, \text{eV}} \, |\vec{E}(v_\perp)| \, . \tag{7}$$

Therefore the sub level density per unit angular frequency results in

$$\rho(\omega) = \frac{n^2 \, N_n}{\Delta E_S / \hbar} = n^2 \cdot \frac{\hbar}{\Delta E_n} = n^5 \frac{\hbar}{13.6 \, eV} \, , \tag{8}$$

independent of the induced Stark field and consequently on the positron velocity. We stress that this density occurs with a motional Stark effect high enough (that is a transverse positronium velocity in a high magnetic field) for producing an interleaving of many n-level fans, and it increases very fast with n. Within the uninteresting region of the transitions to $n < 16$ it is easy to see that the density of sublevels is a constant on n.

The bandwidth $\Delta \lambda_L$ of the second transition laser has to be wider than the Doppler bandwidth $\Delta \lambda_D$ (for Ps cloud efficient covering), and also narrower than $\Delta \lambda_S$ for constraining Ps atom excitation within a reasonable narrow energy band (seeming this suitable for an efficient charge transfer reaction). Therefore the laser energy bandwidth ΔE_L is selected to be smaller than ΔE_S so that the sublevel density of the above equation holds. In these conditions, all the mixed sublevels with transition energy under the laser bandwidth can be populated, at variance with those foreseen by the electric dipole selection rule [10].

In Fig. 2 a schematic picture of the level mixing is shown. The number of levels per unit bandwidth remains, in a crude approximation, unchanged with the increase of the fan aperture because the sublevels lost at the border of the initially chosen laser bandwidth ΔE_L are compensated by the arrival of sublevels coming form the nearby n-states.

The incoherent excitation probability per unit time of the transition $3 \rightarrow$ high–n is

$$W_{3n}(t) = \int_{\Delta E_L} d\omega \, \frac{I(\omega, t)}{\hbar \, \omega} \, \sigma_{3n}(\omega) \tag{9}$$

The absorption cross section $\sigma_{3n}(\omega)$, in this connection, can be recast as

$$\sigma_{3n}(\omega) = \frac{\hbar \, \omega}{c} \, \rho(\omega) \, B_S(\omega). \tag{10}$$

with the absorption coefficient $B_S(\omega)$ appropriate for the excitation of a single sublevel in the quasi–continuum Rydberg level band. By definition this coefficient must be proportional to the square modulus of the electric dipole matrix element:

$$B_S(\omega) \propto |\langle \psi_{n\alpha} | e \, \vec{r} \cdot \vec{\epsilon} | \psi_{31m'} \rangle|^2 \tag{11}$$
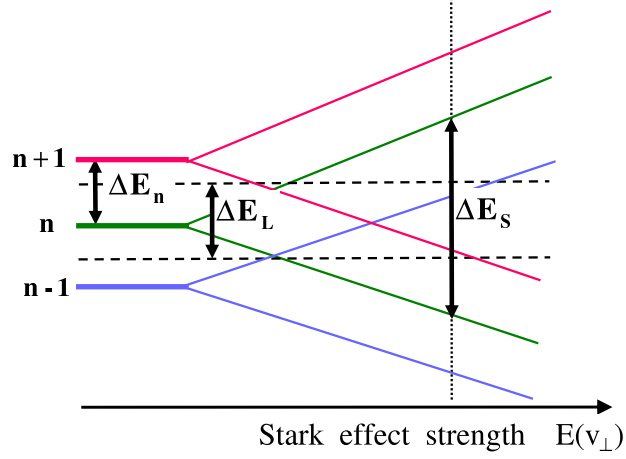
9

FIG. 2: (Color online) Schematic of the level mixing with respect to the laser energy bandwidth ΔE_L, as a function of the strength of the motional Stark electric field ($v_\perp$ is the Ps transverse velocity). The initial n-level is n^2 times degenerate, and its energy distance with the adjacent unperturbed level is ΔE_n. The degeneracy is lifted by the Stark effect and the energy width of the sublevel fan is ΔE_S.

where $\psi_{n\alpha}$ is the wavefunction of a Rydberg sublevel (with ℓ and m mixed) connected by the transition energy $\hbar\omega$ with the low level $\psi_{31m'}$ which is assumed excited by the first laser. The following considerations allows us to estimate magnitude of $B_S(\omega)$. The wavefunction $\psi_{n\alpha}$ relative to the sublevel $n\alpha$ is given by a linear superposition of the n^2 unperturbed wavefunctions with suitable coefficients

$$\psi_{n\alpha} = \sum_{lm} c_{lm}\, \psi_{nlm}. \tag{12}$$

From the normalization condition and assuming a large spreading of $\psi_{n\alpha}$ over the ψ_{nlm}, we get $|c_{lm}| \simeq 1/n$. Using the electric dipole selection rules, which select the final state nlm, we obtain a simple formula connecting $B_S(\omega)$ with the absorption Einstein coefficient for the unperturbed $3 \to$ high–n transition

$$B_S(\omega) \;\propto\; \frac{1}{n^2}\, |\langle \psi_{nlm}|e\,\vec{r}\cdot\vec{\epsilon}|\psi_{31m'}\rangle|^2$$

$$\Rightarrow \quad B_S(\omega) \simeq \frac{1}{n^2}\, B_{3\to n}(\omega) \tag{13}$$

It is worth noting that, because the normalized Rydberg state wavefunctions scale as $n^{-3/2}$ [19], the Einstein coefficient scales as n^{-3} and

$$B_S(\omega) \;\propto\; \frac{1}{n^5}\;. \tag{14}$$

10

This result, together with the level density formula of Eq. (8), brings about the important conclusion that *the absorption probability W_{3n} is practically independent of n and of the transverse Ps velocity.*

Incidentally it is worth noting that Eq. (8) could be straightforwardly written down with the crude argument that a Rydberg level contains n^2 sublevels and the interdistance between n levels is ΔE_n. Anyway, this consideration does not account for the strong sublevel opening and mixing. Within that framework, the above statement on the independence on n of the absorption probability W_{3n} requires a sufficiently wide laser bandwidth (covering several unperturbed n levels), whereas our calculations indicate that this condition is not required.

The strong energy sub-level mixing leads to a physical system with a wide energy bandwidth with uniform energy level distribution. As a consequence, the Doppler effect simply leads to a shift of the resonant frequency for a particular transition within the bandwidth. The above "conservation rule" supports the consideration that for high–n the Doppler effect gives negligible contribution to the global excitation dynamics.

Using Eqs. (8) and (13), and following the procedure and the definitions outlined in the Appendix, the absorption probability rate turns out to be:

$$
\begin{aligned}
W_{3n}(t) &\simeq \int_{\Delta E_L} d\omega \, \frac{I(\omega, t)}{c} \, \frac{B_{3 \to n}(\omega)}{n^2} \, \rho(\omega) \\
&= \frac{I_L(t)}{c} \, n^3 \, B_{3 \to n} \, \frac{\hbar}{13.6 \, \text{eV}} \; .
\end{aligned} \tag{15}
$$

Finally, by considering for definiteness linear laser polarization parallel to the magnetic field direction (hence operating with the selection rule $\Delta m = 0$), we obtain the saturation fluence for the second transition:

$$
F_{sat}(3 \to n) \simeq \frac{c \times 13.6 \, \text{eV}}{B_{3 \to n} \, \hbar \, n^3} \simeq 0.98 \, \text{mJ/cm}^2 \; , \tag{16}
$$

which in fact results approximately a constant in the useful range between $n = 20$ and $n = 30$. We can evaluate the total energy of the laser pulse needed for saturation of this Rydberg excitation with the same method used in the previous subsection, and the result is $E_{II} = 174 \; \mu\text{J}$.

C. The final two–step excitation and its numerical simulation

In the above sections we have found the minimum laser energy requirements to obtain saturation on the two transitions. However, the real Rydberg excitation is performed with

11

near simultaneous laser pulses. This is so because of the narrow useful time window, to cope with a rather large expanding Ps cloud, and the need of avoiding losses on $n = 3$ excited population due to its non negligible spontaneous emission. In this conditions the excitation dynamics involves all the three levels of the two–step transition. If the laser pulse energies are greater than the saturation fluences, an overall level population of 33% is expected for this incoherent excitation [20], in the limit case of no losses. This can be confirmed with a dynamical model as follows.

In the previously discussed picture of the problem there is a lack of information on the exact quantum numbers for the final states of the transition. Therefore we decided to use a simplified excitation dynamics model to obtain an estimate of the high-n state population. We made dynamical simulations considering transitions from $(n, l, m) = (1, 0, 0)$ to the state $(3, 1, 0)$ and from this state to the final states $(n', 2, 0)$ and $(n', 0, 0)$, assuming linear laser polarization as discussed before. In simulations we have considered the total cross section of the transition from the lower to the upper level band substantially equal to the transition cross section between the two levels connected by electric dipole selection rules. This choice is quite usual in problems of this kind [20], and can be inferred from the discussion in the previous subsection.

The resonant Ps excitation is described with a model of multilevel Bloch equation system, derived from a complete density matrix formulation [21], and including for completeness population losses due to spontaneous decay and photoionization for both excited states. Inserting photoionization is necessary for a correct description of the dynamics of Rydberg level population, because this process is in competition with the Rydberg excitation. A rough estimate of the ionization cross sections can be made with the method of Ref. [22]. The ionization probability, proportional to the total energy of the laser pulses, is higher for the sequence $1 \rightarrow 3 \rightarrow$ high–n with respect to the alternative $1 \rightarrow 2 \rightarrow$ high–n, but remains limited to the very small value of 0.3% . In particular, in the case of the second excitation the very long spontaneous emission lifetime and the relatively high ionization cross section make ionization processes responsible for the overwhelming majority of the population loss rate.

Since the laser pulses are substantially incoherent, the light phase in our model is taken as a "random walk" with the step equal to the coherence time. Fig. 3 shows an example of the fractional level populations of Ps as a function of time when irradiated with two simultaneous
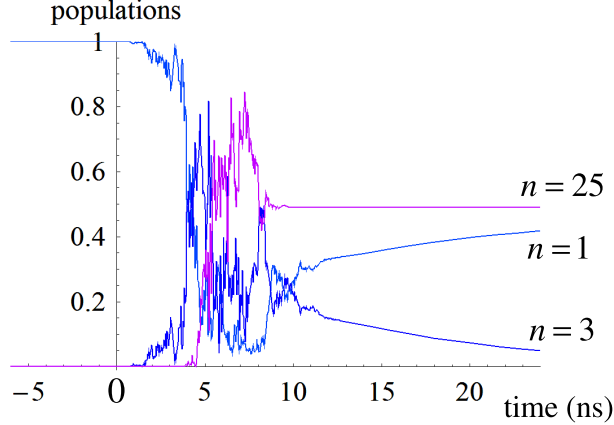
FIG. 3: (Color online) Plot of level populations versus time in a single realization of the excitation process $1 \to 3 \to 25$. The characteristics of the two laser pulses are: (1) time length 4 ns, fluence 200 μJ/cm^2 and spectral width $\Delta\lambda = 0.045$ nm, (2) time length 2 ns, fluence 2.0 mJ/cm^2 and spectral width $\Delta\lambda = 0.72$ nm (two times the Doppler bandwidth), respectively.

laser pulses, the first one resonant with the transition $1 \to 3$ and the second one resonant with the unperturbed transition $3 \to 25$ (specifically $(1, 0, 0) \to (3, 1, 0) \to (25, 2, 0)$). Both pulses have a fluence $F(t)$ (spectral integrated intensity) slightly greater than twice the saturation fluence of the relative transitions, to compensate for population loss. Other characteristics of the pulses are listed in the figure caption.

The final excitation probability for the entire Ps cloud comes from an averaging process over many simulation outputs. The calculation shows that a fraction of about 30% of Ps atoms are excited to the Rydberg state, and this result does not change by irradiating with larger laser fluences, or by considering the slightly less effective transition to the state $(25, 0, 0)$. As a comparison, a parallel numerical simulation can be done in the case of the alternative sequence of excitations $1 \to 2 \to 25$, using the same rules to determine the required laser fluences and bandwidth. An example of the fractional level populations of Ps as a function of time is shown in Fig. 4. The pulses maintain the same time length as before, and the other characteristics are listed in the figure caption. Note that in this case higher energy is required for the second laser pulse. The fraction of excited Ps atoms results around 24%, mainly because the intermediate level suffers an increase in population losses and Doppler bandwidth, which affects the incoherent excitation dynamics with a reduction in average excitation efficiency.
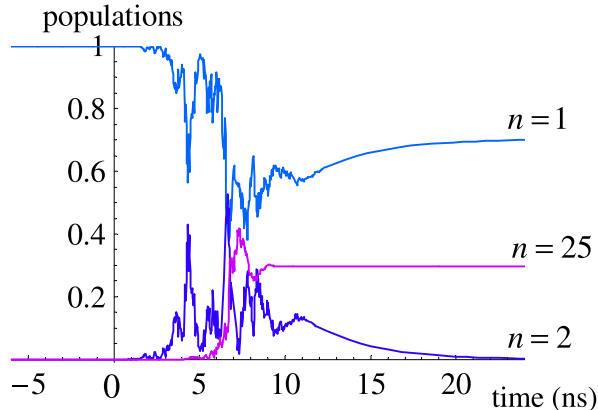
FIG. 4: (Color online) Plot of level populations versus time in a single realization of the alternative excitation process $1 \to 2 \to 25$. The characteristics of the two laser pulses are: (1) time length 4 ns, fluence 25.7 μJ/cm^2 and spectral width $\Delta\lambda = 0.054$ nm, (2) time length 2 ns, fluence 8.0 mJ/cm^2 and spectral width $\Delta\lambda = 0.36$ nm, respectively.

III.   CONCLUSIONS

Excitation process to high-n levels of Ps having 100 K temperature and set in a strong magnetic field presents the peculiarity of a complete re-organization of the energy level structure. In fact, the motional Stark effect splits and totally mixes the otherwise degenerate sublevels of Rydberg states leading to systems with wide energy bandwidth with a uniform energy level distribution. Therefore, Stark effect totally overcomes the Doppler effect in determining the bandwidth of the transition. It is important to note that both effects, Doppler and Stark, depend on the square root of the temperature, hence one expects transition characteristics not to change if the Ps cloud can be extracted from the silica converter with lower average kinetic energy.

The main consequence of the motional Stark effect on the resonant excitation with laser pulses is that it involves a large number of Rydberg states of different n, whose sublevels are interleaved. This theoretical result certainly needs an experimental evidence. Another important consequence of the Stark effect is that the range of high-n levels on which one can obtain high excitation efficiency is limited (for example at $n \leq 27$ for $T = 100$ K) because Ps atoms populating part of the n-sublevels are easily ionized by the induced electric field.

Calculations performed in this paper foresee a 30 % transition efficiency with a tailored laser system (with n below the limit for Stark ionization as discussed before). In particular,

14

the degree of freedom of the interaction bandwidth with the Rydberg level manifold is important to obtain excited Ps atoms in a definite range of energies, which may be required for maximum efficiency of the subsequent charge exchange process with antiprotons. It must be further researched how Ps atoms populating different n–levels, even if with nearby energy values, affect the efficiency of the charge exchange reaction $Ps^* + \overline{p} \to \overline{H} + e^-$.

Simple considerations based on the general theory of radiative transition in atomic physics are used to derive rules which give the laser pulse fluence required for transition saturation. In the first step $1 \to 3$ a relatively simple modeling is sufficient, being the bandwidth essentially Doppler dependent. For the second step $3 \to n$ more attention must be devoted because of the strong motional Stark mixing affecting the Rydberg level structure, resulting in the formula (16).

Finally, we stress that the discussed Ps excitation scheme makes a complete incoherent population transfer, because of the very short coherence length of the two lasers required for the excitation. This is reflected in the maximum excitation efficiency, that cannot be more than 33% [20]. A possible extension of this work towards higher excitation efficiency is the use of coherent population transfer techniques such as STIRAP (STimulated Raman Adiabatic Passage) [23], which appears nevertheless challenging because of the complex structure of the Rydberg levels.

APPENDIX: DEFINITION OF SATURATION FLUENCE

The dynamics of atomic incoherent excitation by a laser pulse can be described by a rate equation model [20]. Considering for definiteness the dipole allowed transition $(n, l, m) = (1, 0, 0)$ to $(n, l, m) = (3, 1, m)$, the rate equation for the high level population P_3 is

$$\frac{dP_3}{dt} = -P_3 \, W_{SE} - P_3 \, W_{31}(t) + P_1 \, W_{13}(t) \tag{A.1}$$

where W_{SE} is the total spontaneous emission rate, $W_{13}(t)$ the absorption probability rate given by Eq. (1), and $W_{31}(t)$ the stimulated emission probability rate. Observing that the 10.5 ns lifetime of the $n = 3$ state is longer than the laser pulse time length which governs the excitation dynamics time scale, for simplicity we discard the spontaneous emission rate, even if the laser pulse duration is not totally negligible compared to it. Therefore it holds $P_1 + P_3 = 1$ for the lower and upper level populations. Assuming that the transition is ruled

by a polarized laser pulse, *i.e.* fixing Δm, we have equal probability for photon absorption and stimulated emission, therefore

$$\frac{dP_3}{dt} \simeq (1 - 2P_3)\, W_{13}(t)\ . \tag{A.2}$$

The excitation is performed with a laser pulse having a total intensity $I_L(t) = \int d\omega\, I(\omega, t)$, where $I(\omega, t)$ is a time–dependent Gaussian spectral intensity resonant with the transition frequency ω_{13}. By selecting the laser broadening equal to Doppler broadening (as required in Section 3.1) and using the fact that the absorption coefficients $B_{1\to3}(\omega)$ of Eq. (2) is in practice a constant, the rate equation (A.2) can easily be solved obtaining

$$P_3(t) = \frac{1}{2}\left[1 - e^{-2F(t)/F_{sat}}\right] \tag{A.3}$$

where

$$F(t) = \int_{-\infty}^{t} dt'\, I_L(t') \tag{A.4}$$

is the laser pulse fluence, and

$$F_{sat}(1 \to 3) = \frac{c\,\sqrt{2}}{B_{1\to3}\, g_D(0)} \tag{A.5}$$

is the saturation fluence. This parameter characterizes the population dynamics: from Eq. (A.3) it is clear that when $F(t) = F_{sat}$ we have 43% of the atoms in the excited state. The maximum excitation, *i.e.* the saturation level of the transition, reaches 50% with high enough pulse energy .

In the case of the second transition, from $(3, 1, m)$ to Rydberg levels, a similar calculation is performed without reference to the Doppler bandwidth and considering that $B_{3\to n}(\omega)$ is essentially a constant over a wide frequency range. The saturation fluence is then given by Eq. (16).

ACKNOWLEDGMENTS

---

[1] R.J. Hughes, Nucl. Phys. A **558**, 605 (1993).

[2] M. Nieto and T. Goldman, Phys. Rep. **205**, 221 (1992).

[3] A. Peters, K.Y. Chung and S. Chu, Nature **400**. 849 (1999).

[4] A. Kellerbauer et al., Nucl. Instr. Meth. B **266**, 351 (2008).

[5] http://doc.cern.ch/archive/electronic/cern/preprints /spsc/public/spsc-2007-017.pdf

[6] E.A. Hessels, D.M. Homan, M.J. Cavagnero, Phys. Rev. A **57**, 1668 (1998); A. Speck, C.H. Storry, E.A. Hessels and G. Gabrielse, Phys. Lett. B **597**, 257 (2004).

[7] D.W. Gidley, H.-G. Peng, R.S. Vallery, Annu. Rev. Mater. Res. **36**, 49 (2006).

[8] F.H.M. Faisal and P.S. Ray, J. Phys. B: At. Mol. Phys. **6**, L715 (1981); A. Karlson and M.H. Mittleman, J. Phys. B: At. Mol. Phys. **29**, 4609 (1996).

[9] L.B Madsen, L.A.A. Nikolopoulos and P. Lambropoulos, J. Phys. B: At. Mol. Phys. **32**, L425 (1999); L.B Madsen, L.A.A. Nikolopoulos and P. Lambropoulos, Eur. Phys. J. D **10**, 67 (2000); L.B Madsen, Nucl. Instr. Meth. B **221**, 174 (2004).

[10] K. P. Ziock, R. H. Howell, F. Magnotta, R. A. Failor and K.M. Jones, Phys. Rev. Lett. **64**, 2366 (1990).

[11] G. Wiebusch et. al., Phys Rev. Lett. **62**, 2821 (1989); J. Main, M. Schwacke and G. Wunner, Phys. Rev. A **57**, 1149 (1998); Yu. E. Lozovik and S. Yu. Volkov, Phys. Rev. A **70**, 023410 (2004); J. Ackermann, J. Shertzer and P. Schmelcher, Phys. Rev. Lett. **78**, 199 (1997), and references therein.

[12] O. Halpern, Phys. Rev. **94**, 904 (1954); G. Feinberg, A. Rich and J. Sucher, Phys. Rev. A **41**, 3478 (1990).

[13] A. Rich, Rev. Mod. Phys. **53**, 127 (1981).

[14] R. H. Garstang, Rep. Prog. Phys. **40**, 8 (1977).

[15] S. M. Curry, Phys. Rev. A **7**, 447 (1973); C. D. Dermer and J. C. Weisheit, Phys. Rev. A **40**, 5526 (1989).

[16] This result can be easily derived from eq. (4) used in the extended discussion over the second transition.

[17] I. I. Sobelman, *Atomic Spectra and Radiative Transitions*, Springer Verlag (1979); H. A. Bethe and E. E. Salpeter, *Quantum Mechanics of One and Two-Electron Atoms*, Plenum, New York, (1977).

[18] W. Gordon, Ann. Phys. (Leipzig), **2**, 1031 (1929); L.C. Green, P.P. Rush and C.D. Chandler, Suppl. Astrophys. J. **3**, 37 (1957).

[19] T. F. Gallagher, Rep. Prog. Phys. **51**, 143 (1988); T. F. Gallagher, *Rydberg Atoms*, Cambridge University Press (2005).

[20] B. W. Shore, *The theory of coherent atomic excitation*, John Wiley & Sons (1990)

[21] P. Meystre and M. Sargent, *Elements of Quantum Optics*, 3rd ed., Springer Verlag(2005).

[22] J. H. Hoogenraad and L. D. Noordam, Phys. Rev. A **57**, 4533 (1998), and references therein.

[23] B.W. Shore et al, Phys. Rev. A **45**, 5297 (1992); K. Bergmann, H. Theuer and B.W. Shore, Rev. Mod. Phys. **70**, 1003 (1998).